Egypt. J. Chem. **Vol. 65,** No. SI:13, pp. 115 – 125 (2022)

Egyptian Journal of Chemistry

http://ejchem.journals.ekb.eg/

Synthesis of TFMs-nanocomposites Based on Cs/TiO_2-Au NPs by PVDC for Degradation of Ethidium Bromide

Amr A. El-Ella [a], Ahmed M. Youssef [b], Hala E. Ghannam [c], Abdallah F. Zedan [a], Gamal E. El-Ghannam [a], Hala M. Ahmed[d] and Al-Sayed A. Al-Sherbini [a*]*

[a]*Department of Laser Applications in Metrology, Photochemistry and Agric., National Institute of Laser Enhanced Science, Cairo University, Giza 12613, Egypt.*

[b] *Packaging Materials Department, National Research Centre, 33 El-Bohouth St. (former El-Tahrir st.), Dokki, Giza, P.O 12622, Egypt.*

[c] *Head of Pollution Laboratory, National Institute of Oceanography and Fisheries, Egypt.*

[d] *Head of Biomedical Equipment Department, Faculty of Applied Medical Science, 6October University.*

Abstract

Ethidium bromide (EtBr), is considered as the one of the first hazards to the environment when discharged into the water drainages with higher permissible levels, it act as a mutagenic interaction with molecular structure of genomic DNA and RNA. Recent studies have focused on surface modification of hydrophobic polymer matrices is an alternative way to change their surface properties. In the present work used the active polymer type of polyvinylidene chloride (PVDC), modified with extracted chitosan and titanium dioxide-(NWs or NPs)-loaded with gold nanoparticles (AuNPs) as a promising thin film-membranes (TFMs)-nanocomposites as PVDC-Cs/TiO_2-(NWs or NPs)-AuNPs, furthermore, a halogen lamp 50 W/m^2 was used with fixed distance 20 cm away from the TFMs nanocomposite to lose mutagenic property of ethidium bromide (EtBr). The synthetic membrane-(TFMs), were characterized by UV-Visible spectra, Fourier transform infrared (FT-IR), X-ray diffraction (XRD) pattern, and transmission electron microscope (TEM). The obtained data exhibited that ~ (80–95) % was degraded with high efficiency within 1 h and with high rates ~ (0.427– 2.75) x10^{-4} mol $dm^{-3}sec^{-1}$ and efficient quantities (Q_e) by mg/g EtBr, within aeration process. The final products of EtBr were detected by HPLC-Chromatography; ~ 75% of EtBr was mineralized within 1 h. thus TFMs-nanocomposites were used efficiently to lose the mutagenesis.
Keywords: TFMs-nanocomposite, Chitosan, TiO_2-NWs, TiO_2/Au-NPs, EtBr, degradation.

1. Introduction

The environmental pollution in terms of water and waste water with pollutant materials, particularly those which are mutagenic in nature and can lead to serious diseases in the wards of cancerous diseases has gained worldwide attention due to the adverse effects on living organisms. Amongst these serious pollutants, ethidium bromide (EtBr) has been considered as carcinogenic pollutant when it is released to the water environment [1]. EtBr, is a dark-red cationic dye that is nonvolatile and moderately soluble in water [2]. EtBr, molecule consists of four aromatic rings and three of these rings can provide strong and specific interaction with molecular structure of genomic DNA and RNA via intercalation between base pairs[3].

Therefore, EtBr is widely utilized as a fluorescent label in molecular biological laboratories by visualization of nucleic acids bands based on gel-electrophoresis technique [4]. But the fact that EtBr is considered as carcinogenic agent originates from its diverse effects on human and animal health which depend on the type of the organism and the exposure level. EtBr can potentially act as a mutagen due to its highly intrinsic binding affinity to nucleic acids leading to deformation of the double-stranded

*Corresponding author e-mail: Amraboelella@rocketmail.com.; (Amr A. El-Ella).
Receive Date: 15 March 2022, **Revise Date:** 24 May 2022, **Accept Date:** 29 May 2022, **First Publish Date:** 29 May 2022
DOI: 10.21608/EJCHEM.2022.127702.5665
©2022 National Information and Documentation Center (NIDOC)

DNA[5].EtBr, constitute one of the first hazards to the environment as it can be normally released into the water environment by discharge it from biological laboratories into water drainages with concentration higher from the mandated permissible levels [6]. The traditional methods for the removal of EtBr relies by mean of treatment of polluted water with lower ratios ~ 10-200 ppm with sodium hypochlorite (bleach) prior to its disposal to drainage [7]. Heterogenous photocatalytic approaches such as the advanced oxidation processes (AOP) have received agreat attention as efficient techniques degradation of organic and inorganic hazardous pollutants from wastewater under natural and light source by illumination with minimal formation of hazard by-products [8].

TiO_2 is considered as one of the most photocatalytic materials for various applications such as the photocatalytic degradation of different toxic compounds in water drains [9-10]. TiO_2 nanoparticles has received tremendous attention in the scientific community because it has proven to be a robust and low cost semiconductor (Sc) material widely investigated in several photovoltaic and photocatalytic applications such as energy conversion using solar cells and chemical degradation. TiO_2 is a nontoxic, inexpensive and stable catalyst that is both biologically and chemically inert [11]. However, the properties of TiO_2 must be modified to enhance the energy conversion efficiency. For example, pristine TiO_2 is featured with a wider bandgap of (3-3.2 eV) which limits its absorption to UV light.

On the other hand, the UV light accounts for only around 5 % of the natural solar spectrum. Thus, exploration of how can TiO_2 be modified to achieve sensitization to visible light of the solar spectrum energy is a significant requisite. To get rid of these limitations recent studies on TiO_2nanoparticles photocatalyst has been used TiO_2-NPs immobilization process as thin film method [12]. The immobilization and stabilization methods, both eliminate the most of these limitations associated with slurries such as particle aggregation and given a self-cleaning and self-sterilizing surfaces [13]. The limitations of TiO_2-NPs comprising the wider optical band gab (3.21eV for anatase) and charge carrier recombination, overcame the limitations by doping TiO_2 with noble metals such as gold nanoparticles (Au-NPs) as heterojunction has been shown as a promising strategy to improve the light harvesting and catalytic properties of TiO_2. The Au-NPs can act as electron trapping centers in addition to the plasmon coupling provided by the strong absorption band of (Au-NPs), in the visible region of the electromagnetic field at around 520 nm. This plasmonic phenomena results from the collective motion and oscillation of free electrons around the metal surfaces, which are called the surface plasmon resonance,(SPR)[14].

In the present work, we have designed (TFMs)-nanocompostes via active of PVDC-(Cs/TiO_2AuNPs), and loaded by TiO_2-NWs and TiO_2-NPs modified by Au-NPs as a promising to lose the mutagenesis of EtBr, under halogen lamp 50 W/m^2. ..

2. Material and Methods

2.1. Materials

Titanium dioxide nanoparticles(TiO_2-deggusa P25), Hydrochloric Acid (HCl), Sodium hydroxide (NaOH), Trisodium citrate ($C_6H_5O_7Na_3$), and polyvinylidene chloride (PVDC) were obtained from (Sigma-Aldrich-USA), Tetrachloroauratetrihydrate ($HAuCl_4$), Ethidium bromide (EtBr), Acetonitrile (CH_3CN), Acetic acid (CH_3COOH) were obtained from Aldrich, (Puriss), Double distilled water was obtained by Millipore instrument.

2.2. Methods

2.2.1. Extraction of chitosan

Extraction process of chitosan from shrimp's wastes was done by three steps and obtained from local markets and suspended it into 4% HCl at 25°C by ratio of 1:14 (w/v) within 36 h then the residual was washed with distilled water to remove the acid and calcium chloride. Firstly deproteinization of shells were done by treating the residual with 5 % NaOH at 90°C for 24 h with a solvent to solid ratio of 12:1 (v/w). After the incubation time the shells were washed with running tap water and sun dried, the product obtained was chitin. The second process to produced chitosan by deacetlyation of obtained chitin [15] by employing with 70 % NaOH solution with a solid to liquid ratio of 1:14 (w/v) and incubated at 25^{0}C for 72 h. The residual was obtained after 72 h washed with running tap water and rinsed with double distilled water. The final product was sun dried and finely grinded to the powder chitosan.

2.2.2. Synthesis of titanium dioxide nanowire (TiO_2-NWs)

TiO_2-NWs were synthesized by hydrothermal methods for treatment of TiO_2nanoparticles (anatase type) with concentrated of KOH solution then acidic treatment by HCl solution. Briefly, 2 g of TiO_2NPs, were added to 40 ml of 10 mol dm^{-3} KOH aqueous solutions in a 100 ml Teflon-vessel. The solution was stirred to 30 min and the Teflon-lined stainless steel autoclaved and putted in an oven at 140°C for 48 h. After the hydrothermal treatment, the precipitate was filtrated and washed (3) times with double distilled water and the precipitate was soaked in an aqueous solution for 2 h at 25°C at favored pH 6. Finally, the precipitate was filtrated and dried in an oven at 80°C

overnight. Dried samples then calcined for 2 h at 450°C with a heating ramp rate of 5° min^{-1}.

2.2.3. Synthesis of TFMs-PVDC/Cs/TiO_2 nanocomposites

80 ml of 0.64 % chitosan (Cs) solution was mixed with 20 ml with active PVDC then added to 80 mg of TiO_2 to obtain the TFMs-PVDC/Cs/TiO_2 loaded by two shapes of TiO_2 then by sonocation the mixture for 10 min, and suspended the mixture into plastic plates with dimensions 15x20 cm. The TFMs-nanocomposites were dried in ambient air to achieve the highly strength and potential rigidity and with thickness about 0.1 mm, was measured by digital micrometer gauge.

2.6. Synthesis of TFMs-PVDC/Cs/TiO_2Au-nanocomposites

One gram of TiO_2-NWs was suspended into 90 ml of double distilled water in standard volumetric flask. 5 ml of 0.5 % sodium citrate solution was added as soon as boiling the mixture started. 1 ml of $5x10^{-3}$mol dm^{-3} $HAuCl_4$ was added by drops with continues stirring. The heating was continues until the color changed to pale pink due formation of Au-NPs on the surface ofTiO_2-NWs. The heating was turning off with continues stirring for 15 min, then the prepared TFMs-nanocomposites were separated by filtration the mixture and drying it at 60ºC to obtain TiO_2/Au-NPs nanocomposite being as pale pink powder. Then, 80 mg of TiO_2/Au-NPs were dispersed in 80 ml of 0.64% chitosan (Cs) solution, then mixed with 20 ml of PVDC by sonocation the mixture for 10 min, then suspended the mixture into plastic plates with dimensions 15x20 cm. The TFMs-PVDC/Cs/TiO_2Au-NPs were dried in ambient air to get highly rigid thin film with thickness about 0.1 mm..

2.2. Characterizations

UV-visible absorbance spectra was measured using JENWAY6800 double beam spectrophotometer and 3 ml of the samples were placed in 1cm, UV–quartzcuvette spectrophotometerand the absorption was recorded within range from 200 – 800 nm. Solution pH was determined by pH meter Systronics 802, India. FT-IR technique made in Germany with range 7500 – 370cm^{-1}, resolution < 1 cm^{-1}, and accuracy < 0.01 cm^{-1} at Micro-Analytical Center, Cairo University, Egypt. XRD, technique, Philips, X'Pert-Pro, and the operation by powder diffractometer operating with a Cu anode with $K\alpha_1$ = 1.54060 Å, $K\alpha_2$ = 1.5444 Å. TEM, analysis, was used for determination the morphology of particle such as shape and size so the prepared thin films were carried out using (JEOL, JEM-1400) at the candidate magnification with an acceleration voltage of 30 kV was used. The aeration bubbles processes were carried out by using peristaltic pump with fixed flow rate of as a source of oxygen. HPLC-Chromotography was used for detection of start and final products of photoreactor, HPLC; 1200, Agilent, Germany equipped with a Zorbax C-18 column (250mm x 94.6 mm x 5 µm) with a diode array detector was used to record the chromatogram. Finally, the halogen lamp 50 W/m^2 (Philips,) was used at fixed distance away from the thin films.

2.7. Photoreactor activity of TFMs-nanocomposites

250 ml of $3x10^{-5}$mol dm^{-3} of fluorescent EtBr, with molecular formula $C_{21}H_{20}BrN_3$, molecular=394.32 g/mole, and absorption peak at λ_{max}= 478 nm, the solution was prepared by dissolving 0.029 g of EtBr in double distilled water was used within the experiments under favored condition at pH10 in basic medium, and then irradiated to light source 50 W/m^2 was placed at fixed distance 20 cm away from the photoreactor. Avoiding the resulting heat by watercirculating path equipped during time course 30 min of experiment. The dark experiment was carried out with TFMs-nanocomposites in absence of halogen lamp. The samples were taken out at regular intervals time ~ 60 min. 3 ml of EtBr solution were taken to monitoring the degradation % and the rates of degradation of EtBr an calculated by equation (1) and (2) and the quantity adsorbate (Qe) of EtBr was calculated by equation (3). The obtained results of TFMs-nanocomposites were measured by using double beam UV/Vis spectrophotometer at 478 nm. The final products of EtBr were detected by using HPLC-chromatography.

3. 3. Result and discussion

3.1 Characterization using TEM

In the study, Fig.(1-a,b,c,d,f) describes the TEM micrographs of the samples, in Fig.(1-a) the chitosan chain extracted from shrimps shells wastes, Fig.(1-b) shown that,the homogenous spherical shapes TiO_2/Au spheres, in the Fig.(1-c) represents TiO_2/Au nanowiresand from the TEM micrographs it clear that, the modification of Au NPs over the surface of $TiO_2$with highly dispersed spherical shape over the TiO_2spheres and nanowires with average size ~ 15 nm. Fig.(1-d) represents Au NPs embedded in TFMs-PVDC/Cs/TiO_2-nanocomposites, Fig.(1-f) represents TiO_2/Au NPs core shell.

3.2 UV–Visible absorption spectra of Au NPs, TiO_2 NPs

UV–Visible absorption spectra of TiO_2 NPs, Au NPs, showed in figure(2), that the optical absorption spectra of 15 nm gold sphers core shell prepared by chemical reduction of $HAuCl_4$, according to turkevich's method [16-17]. As it is well known, the spectrum of the gold spheres has an intense band at 525 nm assignable to the surface plasmon band [17-18]. Such phenomena are attributed to the collective

motion of the electrons in the conduction band. Solving Maxwell's equation for the interaction of radiation field with spherical metal particles under appropriate boundary conditions, it was possible to describe theoretically this effect [19-20]. On the other hand TiO_2 spheres shows broad band with absorption spectra at $\lambda_{max.}$ = 325 nm was specific band for TiO_2 spheres core shell.

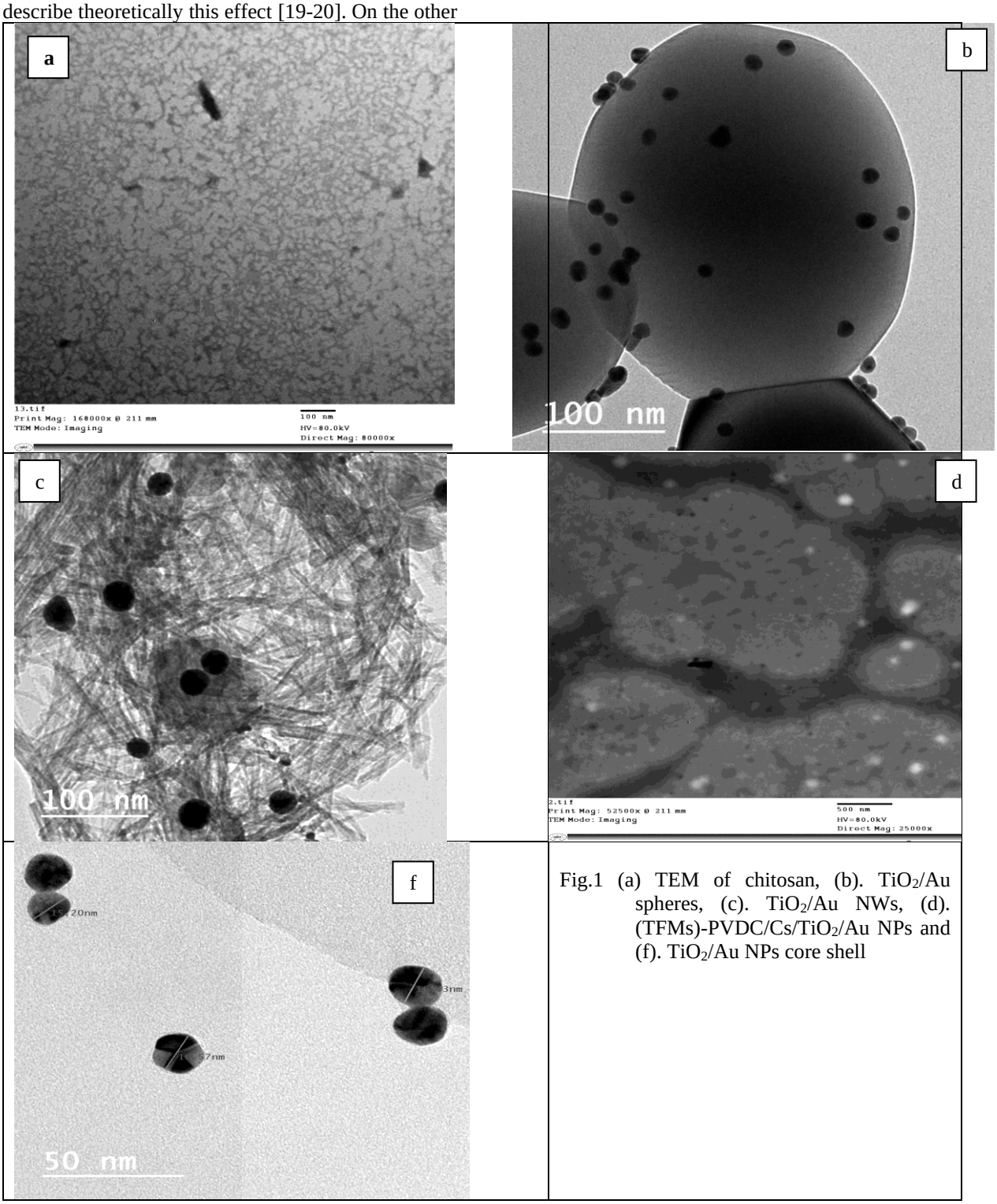

Fig.1 (a) TEM of chitosan, (b). TiO_2/Au spheres, (c). TiO_2/Au NWs, (d). (TFMs)-PVDC/Cs/TiO_2/Au NPs and (f). TiO_2/Au NPs core shell

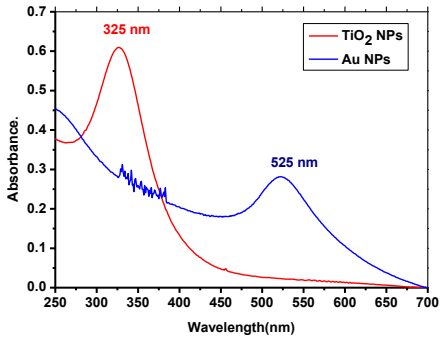

Fig.2 Absorption spectra of Au NPs, TiO_2 NPs

3.3 XRD analysis

The X-ray diffraction pattern of TiO_2 nanoparticle is shown in Fig.3, the peaks of the (101), (116), (103), (200), (213), (105), (107). This corresponds to 25.80°, 38.4°, 48.01°, 54.7° and 63.0°, 69.3°, 75.8° respectively.

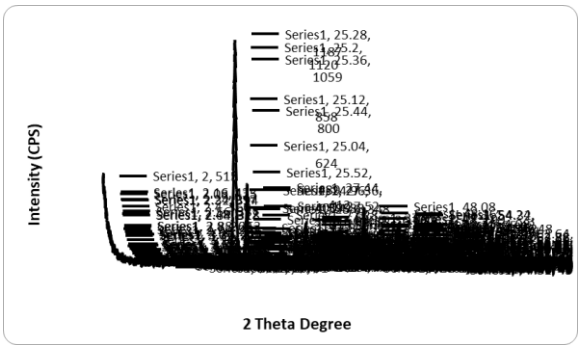

Fig. 3 XRD pattern of TiO_2 nanoparticles

XRD pattern accepted with the JCPDS card no. 21-1272 (anatase TiO_2) and the XRD pattern of TiO_2 nanoparticle other literature. The 2θ at peak 25.8° and 48.01° confirms the TiO_2 anatase type structure. The peaks at 2 h of 25.80° and 48.01° are ascribed to the crystallographic structure of anatase phase indicating TiO_2 anatase phase [21]. There is no any spurious diffraction peak found in the sample.

3.4. FT-IR Spectra

FT-IR Spectra of TiO_2, TiO_2/Au NPs, TiO_2 and TiO_2/Au NWs and biopolymer/CS thin films are shown in Fig.(4-a,b). In the present study, IR spectra of the thin films of TiO_2NPs was showed in Fig.(4-a), it clearly shows three bands. The broadest bandwas observed at 3500 cm^{-1} corresponding to the stretching vibration of the hydroxyl group O-H. The second band is observed around 1605 cm^{-1}, corresponding to bending modes of water Ti-OH and the last band is a prominent peak at 1450 cm^{-1} related to Ti-O modes [22]. In case of TiO_2/Au nanospheres, two characteristic bands at 3693 and 3632 cm^{-1} were detected in the OH spectral region between 3400–4000 cm^{-1}.The bond Ti–OH observed below 3415 cm^{-1} confirms that the existence of hydrogen bonding and attributed to the OH spectral region. It was observed those TiO_2NWs with characteristic peaks in between of 500–700 cm^{-1} and 995 cm^{-1} which are assigned to the Ti–O–Ti and Ti-O stretching vibrations. In order to study the influence of metal capping TiO_2NWs are showed by two characteristic bands at 3793 and 3685 cm^{-1} were detected in the OH spectral region between 3400–4000 cm^{-1}. The shift was observed due to presence of metallic Au loaded on TiO_2NWsalso the absorbance bands of 1625 cm^{-1}, 1390 cm^{-1} and 750 cm^{-1} indicated the presence of molecular functional groups that are responsible for the reduction of Au metal to gold ions. The higher frequency band is ascribed to terminal hydroxyl groups coordinated to Ti^{+4} sites, which are enhance the photocatalytic activity [23]. In Fig. (4-b), the shifting of 1025cm^{-1}, and 1250cm^{-1}, to 1007cm^{-1}, and 1626cm^{-1}, which is corresponding to the C-O stretching this indicates the binding of chitosan to the biopolymer this may be due to the formation of hydrogen bonding. The CH_3 symmetric bending modes which traced 1350cm^{-1} are shifted to 1390cm^{-1}, which is present in chitosan films and absent in the polymer loaded to chitosan films. This clearly indicates that the polymer bind to chitosan by hydrogen bonding. This causes an increase in the bond length, ultimately leading to shift of frequency. The C-N stretching vibration is obtained at 1280cm^{-1}, for plain chitosan thin film, as well as polymer loaded in chitosan. Thus, the FT-IR spectrum supports the

presence of polymer in the chitosan chain as biopolymer/Cs thin film.

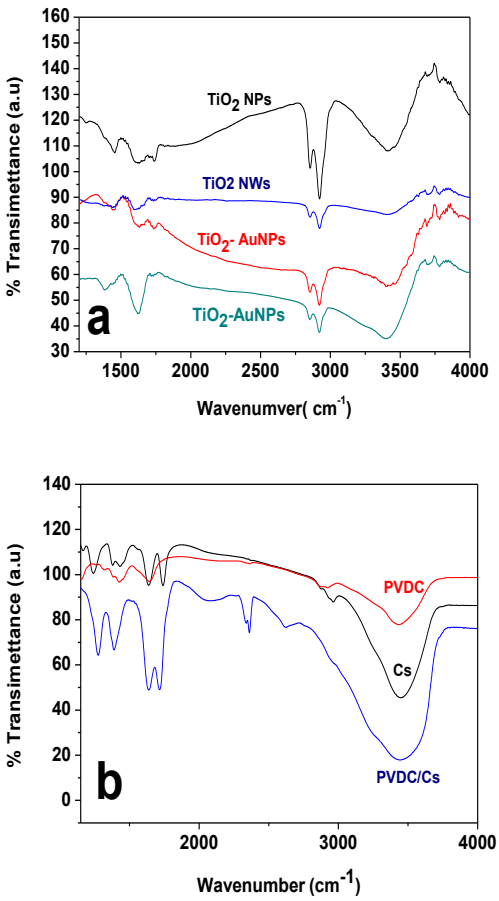

Fig.(4-a,b). FT-IR spectra of TiO_2-(NPs,NWs), TiO_2-(NPs,NWs) Au NPs (a), PVDC/Cs and (Cs) (b)

3.5. Experimental studies

Fig.(5).Shows the electronic absorption spectra of $3x10^{-5}$ mole dm^{-3} of EtBr dye solution was used.

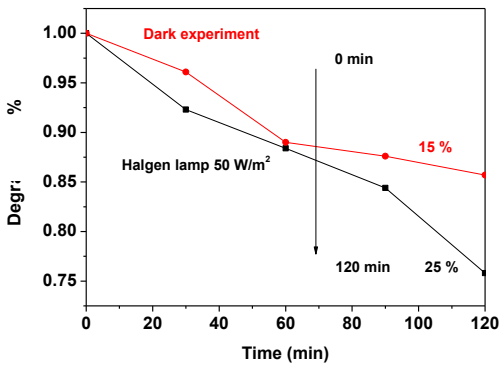

Fig.(5). Dark and light experiment of $3x10^{-5}$ mole dm^{-3} of EtBr

As observed in Fig. (5), the figure showed that, the basic medium at pH10 the solution of EtBr, was placed in dark and under light source 50 W/m^2, the dark experiment indicates that after 2 h only ≈ 15 % of EtBr was adsorbed on the surface of TFMs-nanocomposite, this attributed to adhesion of EtBr over TFMs-surface and becomes limited causing difficulty for the remaining vacant surface sites to be occupied by cationic ions. This is due to the repulsive forces between the positive ions on the solid surface and the liquid phase. In addition to the slightly photodegradation of EtBr was observed after the same interval time course under light source 50 W/m^2, ≈ 25 %was degraded are shown, so the synthesized TFMs-PVDC/CS/TiO_2nanocomposite which have a exhibit photocatalytic activity due to the interference of light reflects through the material and existence of a large number of vacant active binding sites of the synthesized TFMs- nanocomposite [24].

3.6. Photocatalytic studies

80 mg of both tow shapes of TiO_2-(spheres or nanowires)-AuNPs were loaded in TFMs-PVDC/Cs modified by AuNPs over different surface morphologies of TiO_2-anatase structure which have interesting more and efficient strength for degradation of EtBr. The rate of reaction is calculated using the formula described by equation (1).

$$Rate = \Delta[C]/\Delta t \ldots\ldots\ldots\ldots\ldots (1)$$

Where Δ[C] is the change in product concentration by (mol dm^{-3}) during time Δt by (sec). EtBr degradation (%) calculated using equation (2).

$$Degradation (\%) = (A_0 - A / A_0)x100 \ldots\ldots\ldots (2)$$

Where A_0 and A are initial and final concentration respectively.

The quantity adsorbed of EtBr, Q_t (mg/g) at t (min), calculated using equation (3).

$$Q_t = (C_0 - C_t)\ V/M \ldots\ldots\ldots\ldots\ldots\ldots (3)$$

Where C_0 and C_t were the concentrations of EtBr at the initial, the final and time t (min), respectively, M is the mass of EtBr (g) and V is the volume (L).

3.7. Photocatalytic activity of TFMs-PVDC/CS/TiO_2-(Sphere/AuNPs)

In the study the TFMs-PVDC/CS/TiO_2NPs composed with 80mg/20ml of (TiO_2sphere/PVDC) /80 ml of 64% Cs were used for degradation of EtBr. The rate of photocatalytic degradation is strongly influenced with of photocatalyst was used with and no aeration in presence of oxygen and disappearance the rate decreases gradually during period of time. It was observed that, from the results in Fig.(6-a), the degradation rates of EtBr, were increased from (0.427 - 0.908)$x10^{-4}$mol $dm^{-3}$and the efficiency was increased from about (80 – 85)% under no aeration and with aeration respectively, in the period of time. It means that, EtBr solution with $3x10^{-3}$mol dm^{-5} under light source 50 W/m^2 over TFMs-PVDC/CS/TiO_2NPs is efficient degraded with faster rate and with high

efficient quantity (Qt) describe in Fig.(6-b) in case of aeration.

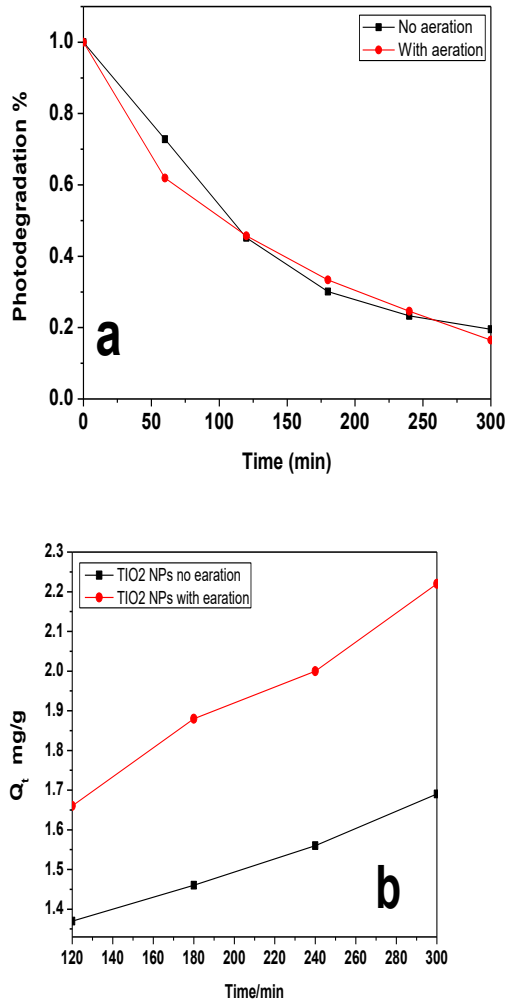

Fig.(6a,b). Photodegradation rates of $3x10^{-5}$ mole dm^{-3} of EtBr, under 50 W/m^2 over TFMs-PVDC/CS/TiO_2 sphere/AuNPs with no aeration (a), and of the quantity of EtBr adsorbed mg/g (b).

The figure illustrated that, the disappearance rate decreases gradually with irradiation time as irradiation time increases. This is might be due to photocatalytic degradation of EtBr. The noble metals influence such gold act as electron traps when deposited over the surface of TiO_2sphere given a faster recombination of active electron/holes must be suppressed and give higher photocatalytic activity of TiO_2. In this case the electrons migrate to Au NPs, and the production of superoxide and hydroxyl radicals were enhanced tending to increase the degradation of EtBr. This was observed that, the degradation of EtBr over TFMs-PVDC/CS/TiO_2-AuNPs no aeration was about $1.23x10^{-4}$mol dm^{-3} with efficiency 83% and increase the rate to $1.38x10^{-4}$mol dm^{-3} with efficient increase to 88% under aeration are showed in Fig.(7,a). Under Visible light irradiation, Au NPs, are photoexcited through the (SPR) absorption then the photoexcited electrons are injected into the surrounding media, in this case, the production of superoxide and hydroxyl radicals are accelerated, which eventually accelerates the degradation rate of EtBr with higher quantity (Qt) shown in Fig.(7,b) in case of aeration and faster rate.

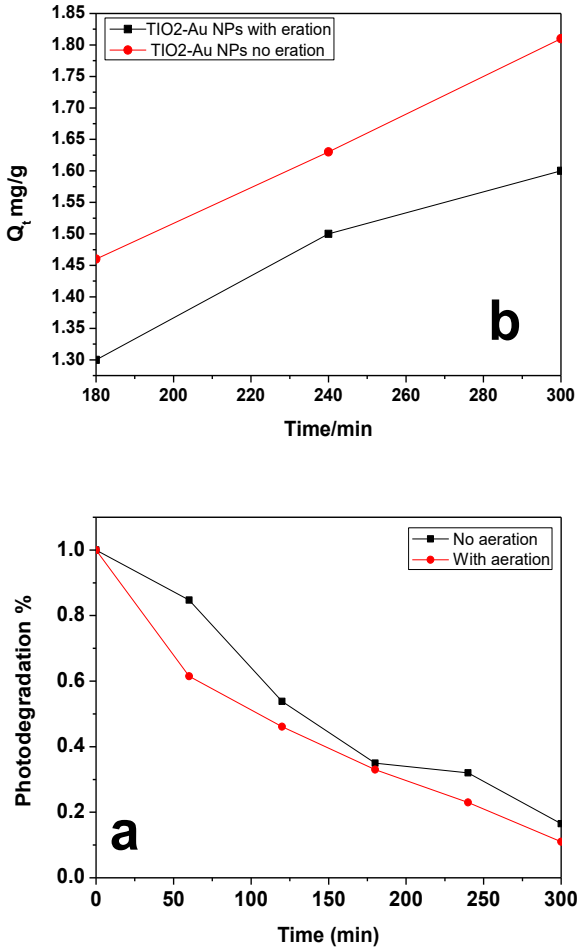

Fig.(7a,b).Photodegradation ratesof $3x10^{-5}$ mole dm^{-3} of EtBr, under 50 W/m^2over over TFMs-PVDC/CS/TiO_2-AuNPs and no aeration (a), and of the quantity of EtBr adsorbed mg/g (b).

3.8. Photocatalytic activity of TFMs-PVDC/CS/TiO_2-NWs

In the present work TiO_2 nanowire (TiO_2-NWs), was used as hierarchical structures have shown to reduce electron/holes pair recombination, which increase the surrounding radicals and might be increasing the photocatalytic efficiency to remove organic and inorganic dyes [25]. Therefore, by using 80 mg of TiO_2-NWs loading in TFMs-PVDC/CS were sufficient to degrade ethidium bromide. Fig.(8 a,b), shows the rates of photodegradation EtBr irradiated at

different intervals time over TFMs-PVDC/CS/TiO_2-NWs with and no aeration.

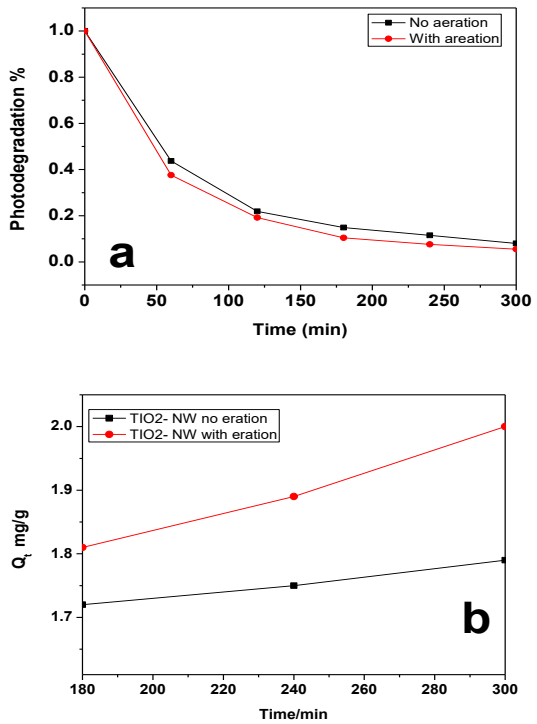

Fig.(8a,b).Photodegradation rates of $3x10^{-5}$ mole dm^{-3} of EtBr, under 50 W/m^2over over TFMs-PVDC/CS/TiO_2-NWs with and no aeration(a), and of the quantity of EtBr adsorbed mg/g (b).

The figure showed that, disappearance rate decreases gradually during irradiation time with increasing the time period due to photocatalytic degradation of ethidium bromide. As expected, the photodegradation rates of EtBr are slightly increase regularly in case of TFMs-PVDC/CS/TiO_2-NWs in case of no aeration with the rate was $2.19x10^{-4}$mol dm^{-3} with 90% degradation. In case of aeration, the rate was increased to $2.37x10^{-5}$mol dm^{-3} with 95% degradation of EtBr more than the rate and % of TFMs-PVDC/CS/TiO_2-(sphers or AuNPs), are concluded in the table (1), and with higher quantity (Qt) shown in Fig.(8,b) in case of aeration.

3.9. Photocatalytic activity of TFMs-PVDC/CS/TiO_2/Au NWs

Deposition of gold NPs (AuNPs) over 80 mg of TiO_2 NWs embedded with TFMs-PVDC/CS, it was found that, Au NPs, act as electron traps accompanying with decreasing of electron/holes recombination keeping a high catalytic activity of TiO_2 NWs. In this case the electrons migrate to Au NPs, associated with the production of superoxides and hydroxyl radical which enhanced tending to increase the degradation of dye. It was observed that, the photodegradation rates of EtBr over the surface of TFMs-PVDC/CS/TiO_2/AuNWs with and no aeration are concluded in the table (1), which illustrated that about EtBr was degraded by rate $2.52x10^{-4}$mol $dm^{-3}$with 91 % degradation with no aeration and in case of aeration the rate was increased to $2.75x10^{-4}$mol $dm^{-3}$with 96% degradation more faster than no aeration, as shown in Fig.(9,a). Under irradiation of light source 50 W/m^2, Au NPs are photoexcited through the surface plasmon resonance (SPR) of metal absorption and photoexcited electrons are injected into the surrounding radicals, then the production of superoxides and hydroxyl radicals are accelerated, which eventually accelerates the degradation rate of dye.

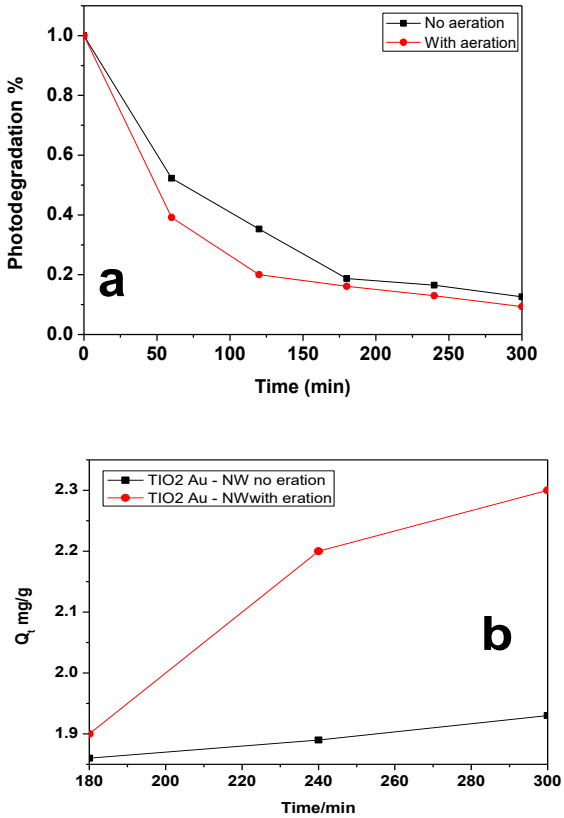

Fig.(9a,b).Photodegradation ratesof $3x10^{-5}$ mole dm^{-3} of EtBr, under 50 W/m^2over over TFMs-PVDC/CS/TiO_2-AuNPs with and no aeration (a), and of the quantity of EtBr adsorbed mg/g (b).

3.10. Proposed mechanism of lose the mutagenic property of EtBr during degradation process

The proposed mechanism of the photocatalytic degradation of dye in aqueous solution in based on biopolymer chitosan TiO_2 or TiO_2/Au NPs thin films

under light source 50 w/m^2 are presented in scheme (1).

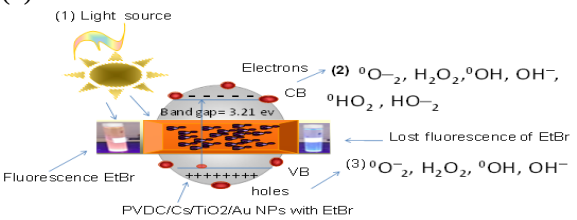

Scheme (1): Schematic diagram of TFM-nanocomposite and the role of radical's scavenger of EtBr

The catalyst absorbs photon which leads to the excitation of electrons from the valence band (VB), to the conduction band (CB), which generates electron/hole pairs. In this case all the system is under reduction oxidation processes. In the reduction process the electrons in the conduction band are captured by oxygen molecules that are dissolved in the medium to produces $^{\cdot}O^{-}_2$, H_2O_2, $^{\cdot}OH$, OH^-, O_2, $^{\cdot}HO_2$ and ,HO^{-}_2 radicals [26]. While in the oxidation process, the holes in the valence band (VB), can be captured by the H_2O or OH^- species that are adsorbed on the surface of the catalyst to produce $^{\cdot}O^{-}_2$, H_2O_2, $^{\cdot}OH$, OH^-, O_2, $^{\cdot}HO_2$ and HO^{-}_2 radicals. All of these radicals having high levels of reactivity and can readily initiate oxidationresulting in the degraded of ethidium bromide dyemolecules. The addition of noble metals like gold over TiO_2 shapes which increases the rate of formation of radicals and accordingly increasing the rate of photocatalytic degradation. The presences of AuNPs, as a trap might be enhance the utilization of visible light by enhance the separation of photogenerated holes and electrons then decreases the electron/holes recompilation.

This leads to high photodegradation and lost it fluorescence of ethidium bromideunder visible light. In addition, in case of nanowire the surface area of the catalyst increases which increasing the radicals in the surrounding accompanying with increasing of the rate ofthe photodegradation by ~ 5 %. To determine the photocatalytic efficiency of TFMs-PVDC/CS quantitatively, the photocatalytic reaction rate constant was obtained by fitting the plots of ln(C_0/C) versus irradiation time t according to the pseudo-first order kinetics under basic pH condition, as shown in Fig.10, and table (1)

The figure shows that after 2 h insignificant adsorption of the control samples ~15 % of EtBr was adsorbed over TFMs-nanocomposites and increased the % to 25 % under light 50 W/m^2. Table (1) showed that, the rates were in between (0.427-2.75) x10^{-4} mole dm^{-3} sec^{-1} and with efficiency from (80 – 95) %. As observed that in table (1), the rate of decomposition assisted by TFMs-PVDC/CS/TiO_2-(NWs/AuNPs), are much faster rate, high (%) of removal efficiency and quantity (Qt) in case aeration than one in case of TFMs-PVDC/CS/TiO_2-(sphere/AuNPs) in compared with TFMs-PVDC/CS/TiO_2-NPs with no aeration.

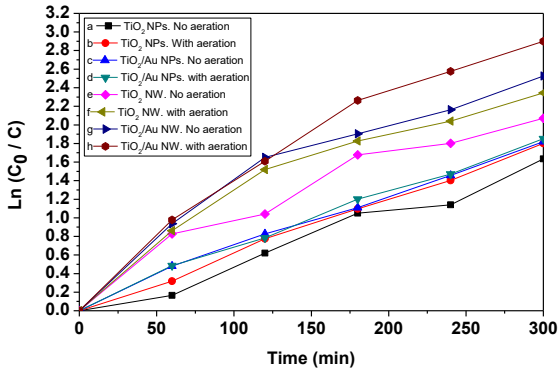

Fig.(10). Normalized curve of EtBr over PVDC/CS/TiO_2 nanocomposites

Table1. Photodegradation percentages and the rates of degradation of EtBr

TFM-PVDC/CS	Photodegradation %	Rates Mol dm^{-3}sec^{-1}
(1) TiO_2 NPs no aeration	80	0.427x10^{-4}
(2) TiO_2 NPs with aeration	85	0.908x10^{-4}
(3) TiO_2/AuNPs no aeration	83	1.23x10^{-4}
(4) TiO_2/AuNPs with aeration	88	1.38x10^{-4}
(5) TiO_2 NWs no aeration	90	2.19x10^{-4}
(6) TiO_2 NWs	95	2.37x10^{-4}
(7) TiO_2/Au NWs no aeration	91	2.52x10^{-4}
(8) TiO_2/AuNWs with aeration	96	2.75x10^{-4}

3.11 HPLC-Chromatographic analysis

In order to identify the intermediates the start and final product of degradation process of the dye under irradiation light source 50 W/m^2. High performance liquid chromatography (HPLC), was employed [10]. Fig.11 presents HPLC, chromatogram standard solution of the dye 3x10^{-5}mol dm^{-3} as the control of the experiment and the end stages final products of dye after degradation process carried out over biopolymer TFMs-PVDC/CS, loaded by two shapes as TFMs-PVDC/CS/TiO_2-(sphere or NWs).

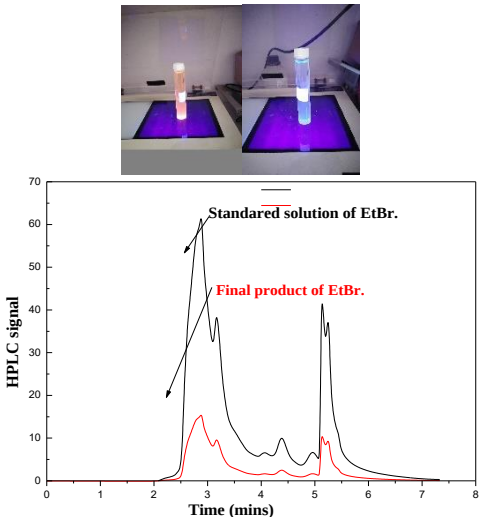

Fig.11.HPLC-Chromatograms ofEtBr irradiated by light source 50 W/m^2 after irradiation time 1 h.

The results showed that, the chromatogram of standard solution of dye gives single peak at retention time 2.82 min, which corresponds to the dye. As irradiation time increases, the intensity of peak decreases, indicating the dye degrades by losing its mutagenic property under irradiation with light source 50 W/m^2 by the reactor was employed, about 75 %, mineralization occurred within 1 h.

4. Conclusions

Photocatalytic degradation of ethidium bromide by TFMs-PVDC/CS/TiO_2-(sphere or NWs) have been carried out in the laboratory scale, the novel photoreactor TFMs-nanocomposites irradiated by light source 50 W/m^2 are more efficient for degradation of of EtBr and loss its mutagenic property at suitable selected PH condition in basic medium was more efficient by TFMs-nanocomposites. Both environmentally and economically by using synthetic TFMs-PVDC/CS consisted of modified by TiO_2, Au/TiO_2-(sphere or NWs) and the TFMs-nanocomposites can be recycled by washing with distilled water and acquired for a longer time period. The final products degrades by about 75 %, of the EtBr was obtained by HPLC-Chromatograms within 1 h. Deposing of Au NPs, over the surface of TiO_2 shapes are improves the catalytic properties of TFMs-nanocomposites. In addition to Improving the photocatalytic properties resulted mainly from the increases of the interfacial charge-transfer process.

5. References

1. Zhang, C., Liu, L., Wang, J., Rong, F., & Fu, D. (2013). Electrochemical degradation of ethidium bromide using boron-doped diamond electrode. *Separation and Purification Technology*, *107*, 91-101.
2. Barros Fernandes Machado, I. M. (2016). Study of the interactions between DNA and ionic liquids.
3. Ge, Z., Sun, T., Xing, J., & Fan, X. (2019). Efficient removal of ethidium bromide from aqueous solution by using DNA-loaded Fe3O4 nanoparticles. *Environmental Science and Pollution Research*, *26*(3), 2387-2396.
4. Law, J. W. F., Ab Mutalib, N. S., Chan, K. G., & Lee, L. H. (2015). Rapid methods for the detection of foodborne bacterial pathogens: principles, applications, advantages and limitations. *Frontiers in microbiology*, *5*, 770.
5. Clark, A. G., Naufer, M. N., Westerlund, F., Lincoln, P., Rouzina, I., Paramanathan, T., & Williams, M. C. (2017). Reshaping the energy landscape transforms the mechanism and binding kinetics of DNA threading intercalation. *Biochemistry*, *57*(5), 614-619.
6. Annapurna, D., Rajkumar, M., & Prasad, M. N. V. (2016). Potential of Castor bean (Ricinus communis L.) for phytoremediation of metalliferous waste assisted by plant growth-promoting bacteria: possible cogeneration of economic products. In *Bioremediation and Bioeconomy* (pp. 149-175). Elsevier.
7. Sharma, S. K. (Ed.). (2015). Green chemistry for dyes removal from waste water: Research trends and applications. John Wiley & Sons.
8. Rahimi, M. R., & Mosleh, S. (2018). Intensification of textile wastewater treatment processes. *Advanced Textile Engineering Materials*, 329-387.
9. Mitsionis, A. I., & Vaimakis, T. C. (2013). The effect of thermal treatment in TiO2 photocatalytic activity. *Journal of thermal analysis and calorimetry*, *112*(2), 621-628.
10. Lavand, A. B., & Malghe, Y. S. (2016). Visible-light photocatalytic degradation of ethidium bromide using carbon-and iron-modified TiO2 photocatalyst. *Journal of Thermal Analysis and Calorimetry*, *123*(2), 1163-1172.
11. Petronella, F., Truppi, A., Striccoli, M., Curri, M. L., & Comparelli, R. (2019). Photocatalytic application of Ag/TiO2 hybrid nanoparticles. In *Noble Metal-Metal Oxide Hybrid Nanoparticles* (pp. 373-394). Woodhead Publishing.
12. Wang, Z., Wang, Y., Zhang, W., Wang, Z., Ma, Y., & Zhou, X. (2019). Fabrication of TiO2 (B)/anatase heterophase junctions at high temperature via stabilizing the surface of TiO2 (B) for enhanced photocatalytic activity. *The*

Journal of Physical Chemistry C, *123*(3), 1779-1789.

13. Rodríguez-González, V. and M. Hinojosa-Reyes, Waste-Porous-Based Materials as Supports of TiO 2 Photocatalytic Coatings for Environmental Applications. Handbook of Ecomaterials, 2018: p. 1-25.
14. Balek, V., Ŝubrt, J., Bountseva, I., Irie, H., & Hashimoto, K. (2008). Emanation thermal analysis study of N-doped titania photoactive powders. *Journal of thermal analysis and calorimetry*, *92*(1), 161-167.
15. Dutta, P.K., J. Dutta, and V. Tripathi, Chitin and chitosan: Chemistry, properties and applications. 2004.
16. Enustun, B. and J. Turkevich, Coagulation of colloidal gold. Journal of the American Chemical Society, 1963. 85(21): p. 3317-3328.
17. Turkevich, J., Colloidal gold. Part II. Gold bulletin, 1985. 18(4): p. 125-131.
18. Link, S. and M.A. El-Sayed, Size and temperature dependence of the plasmon absorption of colloidal gold nanoparticles. The Journal of Physical Chemistry B, 1999. 103(21): p. 4212-4217.
19. Kreibig, U.V., M. , , Optical Properties of Metal Clusters; Springer Series in Material Science. Springer-Verlag: Berlin, 1995. 25: p. 187-201.
20. Bideau, M.C., B.; Dubien, C.; Faure, L.; Kazouan, H. J. Photochem. Photobiol. A: Chem. 1995, 91, 137.
21. Thamaphat, K., P. Limsuwan, and B. Ngotawornchai, Phase characterization of TiO2 powder by XRD and TEM. Kasetsart J.(Nat. Sci.), 2008. 42(5): p. 357-361.
22. Haroun, A.A. and A.M. Youssef, Synthesis and electrical conductivity evaluation of novel hybrid poly (methyl methacrylate)/titanium dioxide nanowires. Synthetic Metals, 2011. 161(19-20): p. 2063-2069.
23. Sun, S. and F. Zhang, Insights into the Mechanism of Photocatalytic Degradation of Volatile Organic Compounds on TiO_2 by Using In-situ DRIFTS, in Semiconductor Photocatalysis-Materials, Mechanisms and Applications. 2016, IntechOpen.
24. Schauer, C. L., Chen, M. S., Chatterley, M., Eisemann, K., Welsh, E. R., Price, R. R., ... & Ligler, F. S. (2003). Color changes in chitosan and poly (allyl amine) films upon metal binding. *Thin Solid Films*, *434*(1-2), 250-257.
25. Wu, W. Q., Rao, H. S., Xu, Y. F., Wang, Y. F., Su, C. Y., & Kuang, D. B. (2013). Hierarchical oriented anatase TiO_2 nanostructure arrays on flexible substrate for efficient dye-sensitized solar cells. *Scientific reports*, *3*(1), 1-7.
26. Swetha, S. and R.G. Balakrishna, Preparation and characterization of high activity zirconium-doped anatase titania for solar photocatalytic degradation of ethidium bromide. Chinese Journal of Catalysis, 2011. 32(5): p. 789-794.